

Layer resolved magnetization dynamics in interlayer exchange coupled $\text{Ni}_{81}\text{Fe}_{19}/\text{Ru}/\text{Co}_{90}\text{Fe}_{10}$ by time resolved x-ray magnetic circular dichroism

T. Martin,^{1,a)} G. Woltersdorf,¹ C. Stamm,² H. A. Dürr,² R. Mattheis,³ C. H. Back,¹ and G. Bayreuther¹

¹Institut für Experimentelle und Angewandte Physik, Universität Regensburg, Universitätsstraße 31, 93040 Regensburg, Germany

²Berliner Elektronenspeicherring-Gesellschaft für Synchrotronstrahlung mbH, Albert-Einstein-Straße 15, 12489 Berlin, Germany

³Institut für Photonische Technologien e.V., Albert-Einstein-Straße 9, 07745 Jena, Germany

(Presented on 8 November 2007; received 13 September 2007; accepted 4 November 2007; published online 6 March 2008)

The magnetization dynamics of each layer of interlayer exchange coupled $\text{Ni}_{81}\text{Fe}_{19}/\text{Ru}(t)/\text{Co}_{90}\text{Fe}_{10}$ films was investigated by time resolved x-ray magnetic circular dichroism (TR-XMCD) after pulsed excitation. The coupling was changed from ferromagnetic to antiferromagnetic by variation of the Ru thickness t . The precessional motion of the individual layers was detected separately by measuring the XMCD signal at the L_3 absorption edge of either nickel or cobalt. From the observation of two frequency components in the precession of both layers in samples with negligible interlayer exchange coupling, the presence of a different coupling mechanism was concluded. Using two different sample geometries, the influence of antiphase and in-phase excitation on the triggered dynamics was studied. © 2008 American Institute of Physics. [DOI: 10.1063/1.2836340]

Ferromagnetic layers coupled by interlayer exchange play a decisive role in modern magnetic memories. In particular, in certain magnetic random access memory cells the “free layer” actually is a synthetic antiferromagnet consisting of two ferromagnetic layers separated by a thin Ru layer which provides strong antiferromagnetic coupling.¹ In giant magnetoresistance (GMR) stacks, interlayer exchange coupling can serve to engineer special properties by coupling, such as switching behavior or strong damping. Due to the increasing writing speeds of these elements, the magnetization dynamics of such coupled bilayers is of special interest. Especially, the influence of the interlayer exchange coupling on precessional modes and damping was investigated in the past by different methods, as (vector network analyzer) ferromagnetic resonance [(VNA)-FMR],^{2,3} pulsed inductive microwave magnetometer,⁴ or Brillouin light scattering.⁵ In contrast to these techniques, the element specificity of x-ray magnetic circular dichroism (XMCD) and the time structure of synchrotron x-ray radiation allow to resolve the magnetization dynamics of a suitable sample for each layer separately, which allows to correlate the precessional dynamics of the coupled layers. This can either be done by time resolved XMCD (TR-XMCD) using pulsed^{6,7} or continuous wave (cw) excitation⁶⁻⁹ and FMR-XMCD,^{10,11} where the longitudinal magnetization component is measured which does not require any time resolution. Recently, Guan *et al.*⁶ have reported decoupled dynamics in a magnetic bilayer with 20 nm thick Cu interlayer using TR-XMCD with pulsed and cw excitations, whereas Arena *et al.*^{8,9} found a weakly coupled motion in a sample with nominally identical structure using TR-XMCD with cw excitation. Here, we demonstrate that layer resolved TR-XMCD measurements using

pulsed excitation can be used to study the influence of interlayer coupling on the precessional motion in coupled bilayers.

The samples were prepared in a ten target ultrahigh vacuum system with a base pressure of 1.5×10^{-8} mbar by dc magnetron sputtering. As demanded by the x-ray transmission experiment, 100 nm thick SiN membranes with $1 \times 1 \text{ mm}^2$ size were used as substrates. The Ta/ $\text{Co}_{90}\text{Fe}_{10}/\text{Ru}/\text{Ni}_{81}\text{Fe}_{19}/M$ (metal M either Al, Ta, or Cu) stacks were patterned as coplanar waveguides by means of optical lithography and lift-off technique. The 350 μm wide central conductor of the waveguide is located on the membrane, whereas the ground conductors are masked by the thick Si frame with $5 \times 5 \text{ mm}^2$ total size (see Fig. 1). This ensures that only the central conductor is measured. During the growth of the magnetic layers, a magnetic field of 100 Oe was applied, which induced a uniaxial magnetic anisotropy with defined easy axis. The easy axis of the $\text{Ni}_{81}\text{Fe}_{19}$

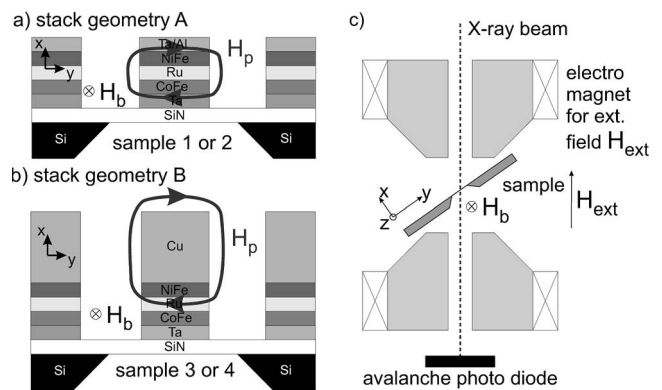


FIG. 1. Stack geometries with pulse field H_p distribution for antiphase (a) and in-phase (b) excitations. (c) Top view of setup (not to scale).

^{a)}Electronic mail: tobias.martin@physik.uni-regensburg.de

(Py) layer is parallel to the waveguide. For the characterization of the samples, conventional FMR,¹² magneto-optic Kerr effect, and VNA-FMR¹³ have been used.

Four different samples will be discussed (the numbers behind the materials denote their thickness in nanometers):

- (1) negligible exchange coupling, anti-phase excitation: SiN/Ta5/Co₉₀Fe₁₀20/Ru10/Ni₈₁Fe₁₉20/Al5;
- (2) negligible exchange coupling anti-phase excitation: SiN/Ta5/Co₉₀Fe₁₀20/Ru2.8/Ni₈₁Fe₁₉20/Ta5;
- (3) ferromagnetic exchange coupling, in-phase excitation: SiN/Ta5/Co₉₀Fe₁₀20/Ru1.4/Ni₈₁Fe₁₉20/Cu100;
- (4) antiferromagnetic exchange coupling, in-phase excitation: SiN/Ta5/Co₉₀Fe₁₀20/Ru0.8/Ni₈₁Fe₁₉20/Cu100.

Additional coupling mechanisms may be present between the layers and may become dominant, as discussed below for samples 1 and 2. By using a 100 nm thick Cu overlayer (samples 3 and 4), the magnetic films are excited in phase, since 97% of the current is carried by the thick Cu layer [Fig. 1(b)]. By omitting the Cu layer, the excitation is antiphase, because the current passes symmetrically through the magnetic stack (samples 1 and 2), see Fig. 1(a). The observed magnetization response confirms the expected excitation modes (see below). In this way, the optic and acoustic precession modes can be selectively excited depending on the stack geometry.

The experiments are done in a pump-probe manner. They were carried out at the BESSY synchrotron radiation source, where x-ray pulses with a full width at half maximum (FWHM) of approximately 70 ps are supplied as probe pulses. By sampling with such pulses and assuming an additional jitter of 40 ps for the electronic devices, the amplitude of the frequency components drops off in a Gaussian manner to 30% at 7 GHz. As a pump pulse, a current pulse from a pulse generator delivering 200 V at 100 ps FWHM with 8 kHz repetition rate is used. It is guided to the sample into the vacuum by high bandwidth coaxial cables. The pulse field amplitude at the sample position decreases linearly with increasing attenuation across the waveguide, which is approximately 6 (10) db from 0 to 6 GHz for the samples with (without) copper overlayer, respectively. The pump pulse is triggered with the storage ring frequency using an appropriate frequency divider and an electronically generated variable delay. The x-ray beam is transmitted through the sample with an angle of 35° with respect to the film normal, passing through the films on the SiN membrane. The transmitted x-ray intensity is measured using a fast Si avalanche photodiode, and gated by a boxcar averager. The tilt axis of the sample is parallel to the waveguide and to the bias field H_b (Fig. 1). Thus, the XMCD signal results from the in-plane y component of the magnetization having the largest relative variation during precession. The XMCD contrast is obtained by subtracting the gated signal for a pumped and an unpumped event. Together with a reference measurement of the static dichroism, where the magnetizations are saturated in the y direction by H_{ext} , an absolute measure for the in plane excursion angle of the magnetization can be obtained.

First, the influence of the stack geometry on the excitation of the individual layers is discussed. Samples 1 and 2

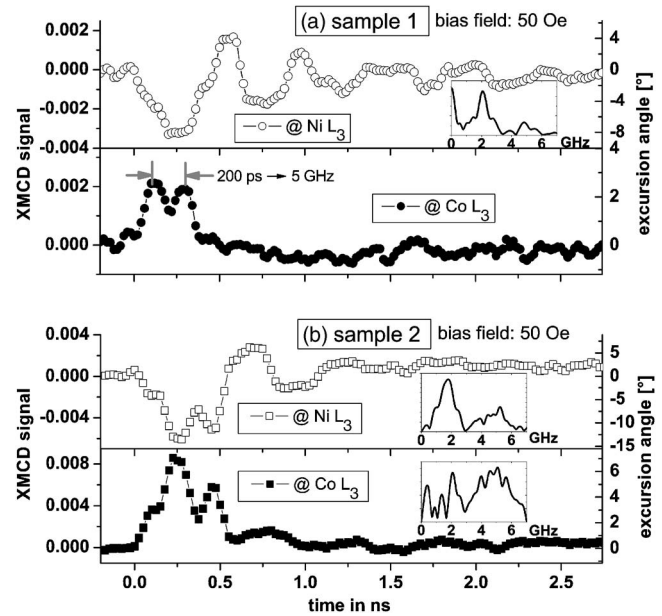


FIG. 2. TR-XMCD precession signal at the Ni and Co L_3 edge of samples 1 (a) and 2 (b) after antiphase excitation at a bias field of 50 Oe. Antiphase excursion of the layers is clearly visible. Insets: FFT, calculated from the data without (a)/after (b) subtraction of the exponential background.

[Figs. 2(a) and 2(b)] both show antiphase excursion caused by the antiphase excitation intended by the stack geometry A [Fig. 1(a)]. On the other hand, the ferromagnetically coupled sample 3 and the antiferromagnetically coupled sample 4 are excited in phase [Figs. 3(a) and 3(b)] using stack geometry B [Fig. 1(b)]. For the ferromagnetically coupled sample 3, the initial excursion and the following precession are both in phase. For sample 4 with antiferromagnetic coupling, this is

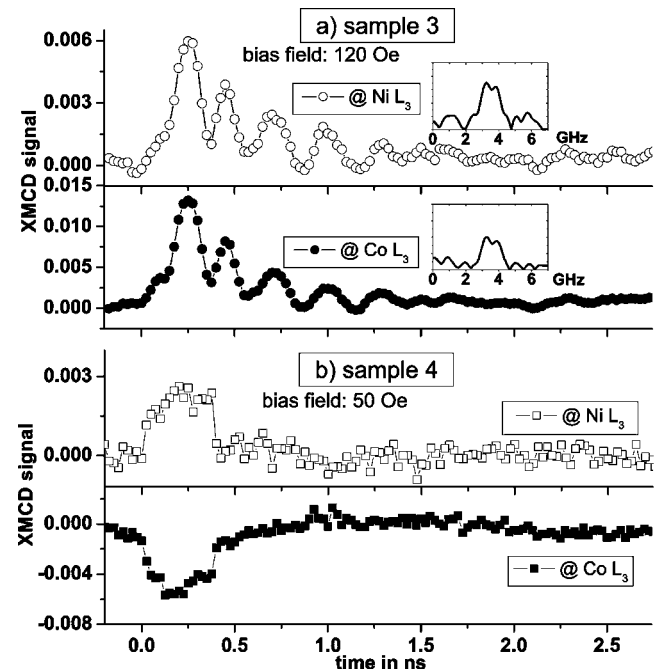


FIG. 3. TR-XMCD precession signal at the Ni and Co L_3 edge of samples 3 (a) and 4 (b) after in-phase excitation at bias fields of 120 and 50 Oe, respectively. Insets: FFT, calculated from the data after subtraction of the exponential background.

different. For this sample, the bias field was chosen in the range, where the layer magnetizations are oriented antiparallel to each other. This was verified by layer resolved hysteresis loops using static XMCD. At this field, the precession frequency was too high to be resolved, but the first excursion of the magnetization clearly shows an antiphase motion. Because of the in-phase initial excitation, this can only be caused by the antiferromagnetic coupling; otherwise, both layers would show in-phase excursion.

Next, the influence of the coupling on the precessional motion of the individual layers of the samples is discussed. For all the samples an exponentially decaying XMCD background signal is observed with a decay time comparable to the precessional decay time. This background signal becomes more pronounced with increasing magnetic stiffness [compare Fig. 3(a)]; its origin is still unclear. For samples 2 and 3, it was subtracted from the measured data before the Fourier transformation. For all presented samples, a small reflection of the main exciting pulse arriving at $t=1.5$ ns leads to a second excitation resulting in a distortion of the initial precession.

At a bias field of 50 Oe, the $\text{Co}_{90}\text{Fe}_{10}$ layer of sample 1 [Fig. 2(a)] shows a strongly damped precession at about 5 GHz. The $\text{Ni}_{81}\text{Fe}_{19}$ layer has its main oscillation frequency at approximately 2 GHz and a very weak oscillation at approximately 5 GHz. Although the magnetic layers are certainly not exchange coupled, there may be very weak dipolar coupling leading to the 5 GHz component in the $\text{Ni}_{81}\text{Fe}_{19}$ signal. Similar trends have been reported by Arena *et al.*^{8,9} The excursion angle for the $\text{Co}_{90}\text{Fe}_{10}$ layer is smaller than for the $\text{Ni}_{81}\text{Fe}_{19}$ layer because of its higher anisotropy and stiffness.

For sample 2 [Fig. 2(b)], the excitation angles are larger compared to sample 1 because of a somewhat lower pulse attenuation. In comparison to sample 1, the coupling-induced mutual influence of the magnetization dynamics of both layers is more pronounced in sample 2. This suggests that dipolar coupling is somewhat stronger in this sample. In contrast to sample 1, the $\text{Ni}_{81}\text{Fe}_{19}$ magnetization of sample 2 is performing a large amplitude high frequency motion at 375 ps corresponding to the motion of the $\text{Co}_{90}\text{Fe}_{10}$ magnetization. While the $\text{Co}_{90}\text{Fe}_{10}$ layer of sample 1 does not show any well-defined signal beyond 600 ps, a forced oscillation of the $\text{Co}_{90}\text{Fe}_{10}$ with the precession frequency of $\text{Ni}_{81}\text{Fe}_{19}$ (≈ 2 GHz) is seen in sample 2 due to dipolar coupling. Although these low frequency oscillations of the two layers start 180° out of phase due to the stack geometry A, the phase difference decreases in time reaching approximately 90° after about 800 ps. This suggests ferromagnetic Néel coupling, which favors in-phase precession. Such time dependent processes cannot be observed when cw excitation is used and demonstrate the strength of pulsed excitation. The effect of the coupling on the decay time of the individual layers could not be determined with sufficient accuracy due to the relatively low signal-to-noise ratio (SNR). The bias

field dependence of the obtained frequencies agrees with the behavior observed by VNA-FMR within the error margin.

In Fig. 3(a) the layer resolved precession of sample 3 with strong ferromagnetic exchange coupling is shown. Compared to samples 1 and 2, both of the strongly coupled layers nearly follow the same precessional motion. The fast Fourier transform (FFT) shows a broad peak around 3.5 GHz in the signal of each layer, corresponding to the acoustical mode, which is excited much more strongly by stack geometry B than the optical mode which is not observable, because of its high frequency and low amplitude.

Summarizing, we have shown how the element-specificity of x-ray magnetic circular dichroism together with the time resolution given by the synchrotron x-ray pulses can be used for a separate detection of the dynamics of interlayer exchange coupled magnetic bilayers. In this way the two precessional frequencies of a weakly coupled $\text{Ni}_{81}\text{Fe}_{19}/\text{Ru}/\text{Co}_{90}\text{Fe}_{10}$ system could be detected in *each* magnetic layer. Furthermore, we have shown how to change from in-phase to antiphase excursion in a bilayer using two different stack geometries. Experiments using layer resolved TR-XMCD with cw excitation allowing for a more accurate determination of the damping via the linewidth of resonance curves will be presented in a forthcoming paper.

Support by the Deutsche Forschungsgemeinschaft (DFG SPP1133) and BMBF (05 ES3XBA/5) is gratefully acknowledged. The authors want to thank T. Kachel for his support at the BESSY beamline, D. Weiss for the access to the clean-room facilities, and H. Stoll for the supply with sample holder waveguides.

¹B. N. Engel, J. Akerman, B. Butcher, R. W. Dave, M. DeHerrera, M. Durlam, G. Grynkeiwich, J. Janesky, S. V. Pietambaram, N. D. Rizzo, J. M. Slaughter, K. Smith, J. J. Sun, and S. Tehran, *IEEE Trans. Magn.* **41**, 132 (2005).

²B. K. Kuanr, M. Buchmeier, D. E. Bürgler, and P. Grünberg, *J. Appl. Phys.* **91**, 7209 (2002).

³J. Lindner and K. Baberschke, *J. Phys.: Condens. Matter* **15**, S465S478 (2003).

⁴T. Martin, M. Belmeguenai, M. Maier, K. Perzlmaier, and G. Bayreuther, *J. Appl. Phys.* **101**, 09C101 (2007).

⁵B. K. Kuanr, M. Buchmeier, R. R. Gareev, D. E. Bürgler, R. Schreiber, and P. Grünberg, *J. Appl. Phys.* **93**, 3427 (2003).

⁶Y. Guan, W. E. Bailey, C.-C. Kao, E. Vescovo, and D. A. Arena, *J. Appl. Phys.* **99**, 08J305 (2006).

⁷A. Puzic, B. Van Waeyenberge, K. Wei Chou, P. Fischer, H. Stoll, G. Schütz, T. Tyliczszak, K. Rott, H. Brückl, G. Reiss, I. Neudecker, T. Haug, M. Buess, and C. H. Back, *J. Appl. Phys.* **97**, 10E704 (2005).

⁸D. A. Arena, E. Vescovo, C.-C. Kao, Y. Guan, and W. E. Bailey, *Phys. Rev. B* **74**, 064409 (2006).

⁹D. A. Arena, E. Vescovo, C.-C. Kao, Y. Guan, and W. E. Bailey, *J. Appl. Phys.* **101**, 09C109 (2007).

¹⁰G. Boero, S. Rusponi, P. Bencok, R. S. Popovic, H. Brune, and P. Gambardella, *Appl. Phys. Lett.* **87**, 152503 (2005).

¹¹J. Goulon, A. Rogalev, F. Wilhelm, N. Jaouen, C. Goulon-Ginet, G. Goujon, J. Ben Youssef, and M. V. Indenbom, *JETP Lett.* **82**, 696 (2005).

¹²M. Belmeguenai, T. Martin, G. Woltersdorf, M. Maier, and G. Bayreuther, *Phys. Rev. B* **76**, 104414 (2007).

¹³I. Neudecker, G. Woltersdorf, B. Heinrich, T. Okuno, G. Gubbiotti, and C. H. Back, *J. Magn. Magn. Mater.* **307**, 148 (2006).